STRUCTURE-BASED RESOLUTION OF TURBULENCE FOR SODIUM FAST REACTOR THERMAL STRIPING APPLICATIONS

Michael J. Acton, Giancarlo Lenci, Emilio Baglietto
Department of Nuclear Science and Engineering
Massachusetts Institute of Technology
77 Massachusetts Avenue, Cambridge, MA 02139, USA
actonm@mit.edu, lenci@mit.edu, emiliob@mit.edu

ABSTRACT

Thermal striping in sodium fast reactors (SFR) is characterized by oscillatory mixing of non-isothermal sodium coolant streams, and is a potential cause of thermal fatigue damage in upper-plenum materials. Accurate simulation of thermal striping is essential to support both reactor design and operation, but it is severely constrained by CPU requirements and uncertainty introduced by turbulence closures. Unsteady Reynolds-averaged Navier-Stokes (URANS) models are incapable of providing a reasonable level of description of flow fields, including variances and fluctuation spectra. Those parameters are needed to understand and mitigate the effects of thermal striping. Large-eddy simulation (LES) models are computationally restrictive for typical high-Reynolds-number reactor flow applications. Here, the performance of a recently developed structure-based (STRUCT) hybrid URANS/LES turbulence approach in predicting thermal striping is assessed on a triple-jet water case. The STRUCT approach is characterized by the identification of flow regions where the scale-separation assumption of URANS is not met. In those regions, partial resolution of turbulence is applied. Unresolved scales in the fully resolved and partially resolved regions are treated with a nonlinear eddy-viscosity model. The goal is to assess the robustness of the STRUCT approach for simulations of thermal striping. STRUCT demonstrated LES-like accuracy on computational grids typical of URANS simulations, reproducing experimental profiles and dominant temperature fluctuation frequencies. A reduction in computational cost of 70 times was achieved over LES, while maintaining the reliable grid-convergence behavior of URANS.

KEYWORDS
Turbulence modeling, Thermal striping, Hybrid URANS/LES, STRUCT, Sodium fast reactors

1. INTRODUCTION

The high core-power density and coolant thermal conductivity in sodium fast reactors (SFR) can lead to the undesirable occurrence of thermal striping. The phenomenon is characterized by the turbulent mixing of sodium streams at different temperatures. This produces cyclic thermal loads in materials that may cause thermal fatigue failure, as in the case of the coolant leaks which occurred at both the Phénix and the Superphénix sodium fast reactors [1].

Thermal striping was identified as a potential issue for sodium fast reactors in the 1970s, and was first investigated by Brunings [2] in a sodium mixing tank. Experiments conducted by Tenchine and Nam [3], Moriya and Ohshima [4], Hattori et al. [5], Wakamatsu, Nei, and Hashiguchi [6] focused on the macroscopic behavior of the fluid. Moriya and Ohshima [4] determined that sufficient similarity exists between sodium

and water in thermal striping tests for Reynolds numbers exceeding 2.0×10^4 and for Péclet numbers exceeding 6.0×10^2.

Experiments conducted by Kawamura et al. [7], Yuki et al. [8], and others focused on the thermal striping behavior in T-junction pipes. Hu and Kazimi [9], Kamide et al [10], and Lee et al. [11] performed numerical analyses based on those experiments. Chellapandi, Chetal and Raj [12] determined material limits in different parts of the reactor core in terms of temperature fluctuation intensity and frequency, while Wakamatsu, Nei, and Hashiguchi [6] studied the thermal response mechanism in materials exposed to temperature fluctuations.

Numerical analyses performed based on the early experiments indicated that the lumped-parameter approach is intrinsically unable to capture the local, three-dimensional fine-scale fluctuations characteristic of thermal striping. More recent experiments, such as the triple jet of Tokuhiro and Kamide [13] and Choi and Kim [14], have therefore been designed to support the development and validation of more advanced numerical simulations using computational fluid dynamics (CFD). These experiments have a finer measurement resolution, and are restricted to small geometric domains. Recent experiments, such as Crosskey and Ruggles [15], Olumuyiwa, Skifton and Tokuhiro [16], Lu, Cao, and Xiao [17], and Lomperski et al. [18] utilized increasingly accurate measurement techniques like laser Doppler velocimetry (LDV), particle image velocimetry (PIV), and high-speed infrared cameras for the determination of the three-dimensional temperature and velocity fields.

The CFD analyses of triple-jet flow experiments performed by Nishimura et al. [19] and Kimura, Nishimura, and Kamide [20] have shown limitations in the description of thermal striping when using the standard k-ε Reynolds-averaged Navier-Stokes (RANS) turbulence model. Nishimura and Kimura [21], have evidenced limited improvement in capturing mean flow profiles and overall oscillatory motion through the use of a newly developed low-Reynolds number stress and heat flux model (LRSFM). Choi and Kim [14] indicated a limited level of success when adopting the Shear Stress Transport (SST) and Elliptic Relaxation models.

In general, RANS and unsteady RANS (URANS) approaches show a fundamental lack of applicability to thermal striping due to the complex non-periodic nature of the flow structures present. On the other hand, large-eddy simulation (LES) models have shown great success in triple-jet cases, as evidenced by Cao, Lu, Lv [22] and Jung and Yoo [23]. Though LES models are able to capture the fundamental unsteadiness of thermal striping, they are computationally restrictive for full-scale simulations. This underpins the motivation for turbulence models that could combine low cost, robustness and accuracy, which is the goal of hybrid URANS/LES approaches.

In the present study, we assess the performance of a recently developed structure-based (STRUCT) hybrid turbulence approach [24] in simulating thermal striping. The foundation of the approach is an anisotropic nonlinear eddy-viscosity k-ε model with a cubic stress-strain relation [25]. On top of such cubic model, STRUCT enables a partially resolved hybrid formulation in selected turbulent structures. Model-enabling locations are identified as regions where the scale-separation assumption of URANS is not met, due to strong flow deformation. In those locations, the amount of locally modeled turbulent kinetic energy is reduced and more scales of turbulence are resolved. The selection of model-enabling regions is made using a formulation based on characteristic flow frequencies. Here, the effectiveness of the approach has been assessed, by using flow-dependent parameters, while the complete formulations will be tested in future work.

To demonstrate the applicability of STRUCT for the thermal striping case, the model is applied to simulate the Tokuhiro and Kimura [13] triple-jet experiment. An emphasis is made to compare simulation results to the experiment in terms of accurate prediction of temperature, temperature fluctuation, and velocity profiles

throughout the domain. In addition, the ability of the model to capture the oscillatory non-periodic nature of the flow, and to determine the frequency of the flow fluctuations is evaluated. Among the studied quantities, the magnitude, profile, and frequency of temperature fluctuations are of utmost importance due to the direct effect on the thermal loads in structural materials, which can lead to fatigue and failure.

Results show that the STRUCT model accurately describes the time-averaged flow behavior on coarse grids and reasonably predicts the frequency of temperature fluctuations. This represents a 70x speedup over LES, and significant increase in flow description compared to URANS. While the capabilities of the STRUCT approach have been demonstrated in this work, a complete formulation is currently being finalized and will be evaluated in the future.

2. TURBULENCE MODELLING

In this section, the mathematical formulations of the turbulence models tested in this work on the triple-jet test case are briefly described. All equations in this paper assume incompressible Newtonian flow.

Many turbulence models, though differing in mathematical derivations, share strong similarities in their basic equations [26]. Let us introduce equations that are valid for the turbulence models introduced in the sub-sections below.

The velocity field u_i is decomposed as the sum of a resolved $\bar{u}_i$ and a residual u_i' term. A similar decomposition is done for pressure. Such decomposition is obtained through a statistical operation, marked with an overbar, that commutes with differentiation in space and time [27]. Applying the operation to the momentum and mass conservation Navier-Stokes equations, we obtain the resolved equations:

$$\frac{\partial \bar{u}_i}{\partial t} + \bar{u}_j \frac{\partial \bar{u}_i}{\partial x_j} = -\frac{1}{\rho}\frac{\partial \bar{p}}{\partial x_i} + \nu \frac{\partial^2 \bar{u}_i}{\partial x_j \partial x_j} - \frac{\partial \tau_{ij}}{\partial x_j}, \quad \frac{\partial \bar{u}_j}{\partial x_j} = 0 \tag{1}$$

The equations (1) are equivalent to those where the velocity and pressure fields are instantaneous, except for the last term in the momentum equation. This term contains the residual stress tensor, expressed as:

$$\tau_{ij} = \overline{u_i u_j} - \bar{u}_i \bar{u}_j \tag{2}$$

Term τ_{ij} needs to be closed, and closure models tested in this work are shown in the paragraphs below.

2.1. Realizable *k-ε*

While the standard *k-ε* model [28][29], has long been the industry workhorse, most recently the variant proposed by Shih et al. [30] has demonstrated improved predictions and has been widely adopted for internal flow applications. The model enforces realizability and, most importantly, introduces sensitivity to vortex stretching and dissipation. The residual stress anisotropy tensor a_{ij} is defined, as typically done in linear closures, through the Boussinesq approximation as in (3). The turbulence eddy viscosity has the same form as in the standard *k-ε*, which is show in (4).

$$a_{ij} = \tau_{ij} - \frac{2}{3}k\delta_{ij} = -2\nu_t \bar{S}_{ij} \tag{3}$$

$$\nu_t = C_\mu \frac{k^2}{\varepsilon} \tag{4}$$

Realizability is enforced in the model through a variable formulation of the C_μ coefficient, as in (5).

$$C_\mu = \frac{1}{A_0 + A_s \frac{kU^*}{\varepsilon}} \tag{5}$$

Where parameter U^* is commonly implemented as:

$$U^* = \sqrt{\bar{S}_{ij}\bar{S}_{ij} + \bar{\Omega}_{ij}\bar{\Omega}_{ij}} \tag{6}$$

The mean strain rate tensor and mean rotation rate tensor are defined as:

$$\bar{S}_{ij} = \frac{1}{2}\left(\frac{\partial \bar{u}_\iota}{\partial x_j} + \frac{\partial \bar{u}_j}{\partial x_i}\right) \ , \bar{\Omega}_{ij} = \frac{1}{2}\left(\frac{\partial \bar{u}_i}{\partial x_j} - \frac{\partial \bar{u}_j}{\partial x_i}\right) \tag{7}$$

and coefficients in (5) are $A_0 = 4$ and:

$$A_s = \sqrt{6}\cos\left(\frac{1}{3}\text{acos}\left(\sqrt{6}\bar{S}_{ij}\bar{S}_{jk}\bar{S}_{ki}\left(\bar{S}_{ij}\bar{S}_{ij}\right)^{-1/3}\right)\right) \tag{8}$$

For the sake of brevity, we do not report here the modified equation for ε, which is available in [30].

2.2. Nonlinear eddy-viscosity model

Boussinesq eddy-viscosity models rely on a linear relation between residual anisotropic stresses and strains in the resolved flow field. This simple relation is believed to inaccurately describe the momentum transfer between the residual and the resolved field. Pope [31] proposed a more general nonlinear eddy-viscosity model (NLEVM) formulation. Residual anisotropic stresses are provided by a polynomial formulation which is function of k, ε, and various invariants derived from the resolved velocity gradient tensor.

Among the NLEVM closures that have been proposed in the literature, here we select the cubic formulation of Baglietto and Ninokata [25][32], which is based on the original proposal of Shih, Zhu and Lumley [33]. Such model was developed in order to achieve general robustness and improved description of anisotropy in several test cases, including flow in nuclear fuel bundles. In the model, the residual stress anisotropy tensor is defined as follows:

$$\begin{aligned} a_{ij} = \tau_{ij} - \frac{2}{3}k\delta_{ij} = -2\nu_t\bar{S}_{ij} + 4C_1\nu_t\frac{k}{\varepsilon}\left[\bar{S}_{ik}\bar{S}_{kj} - \frac{1}{3}\delta_{ij}\bar{S}_{kl}\bar{S}_{kl}\right] + 4C_2\nu_t\frac{k}{\varepsilon}\left[\bar{\Omega}_{ik}\bar{S}_{kj} + \bar{\Omega}_{jk}\bar{S}_{ki}\right] \\ +4C_3\nu_t\frac{k}{\varepsilon}\left[\bar{\Omega}_{ik}\bar{\Omega}_{jk} - \frac{1}{3}\delta_{ij}\bar{\Omega}_{kl}\bar{\Omega}_{kl}\right] + 8C_4\nu_t\frac{k^2}{\varepsilon^2}\left[\bar{S}_{ki}\bar{\Omega}_{lj} + \bar{S}_{kj}\bar{\Omega}_{li}\right]\bar{S}_{kl} \\ + 8C_5\nu_t\frac{k^2}{\varepsilon^2}\left[\bar{S}_{kl}\bar{S}_{kl} + \bar{\Omega}_{kl}\bar{\Omega}_{kl}\right]\bar{S}_{ij} \end{aligned} \tag{9}$$

The transport equations for k and ε, shown in (10) and (11), are those of the standard k-ε model, where the coefficients recommended by Launder and Spalding [29] are used as: $C_{\varepsilon 1} = 1.44$, $C_{\varepsilon 2} = 1.92$, $\sigma_k = 1.0$, $\sigma_\varepsilon = 1.3$. The production term P_k is formulated as in (12).

$$\frac{\partial k}{\partial t} + \bar{u}_j\frac{\partial k}{\partial x_j} = \frac{\partial}{\partial x_j}\left[\left(\nu + \frac{\nu_t}{\sigma_k}\right)\frac{\partial k}{\partial x_j}\right] + P_k - \varepsilon \tag{10}$$

$$\frac{\partial \varepsilon}{\partial t} + \bar{u}_j \frac{\partial \varepsilon}{\partial x_j} = \frac{\partial}{\partial x_j}\left[\left(\nu + \frac{\nu_t}{\sigma_\varepsilon}\right)\frac{\partial \varepsilon}{\partial x_j}\right] + C_{\varepsilon 1}\frac{\varepsilon}{k}P_k - C_{\varepsilon 2}\frac{\varepsilon^2}{k} \tag{11}$$

$$P_k = 2\nu_t \bar{S}_{ij}\bar{S}_{ij} \tag{12}$$

The following parameters describe the resolved rotation and strain in a dimensionless fashion:

$$\bar{S}^* = \frac{k}{\varepsilon}\sqrt{2\bar{S}_{ij}\bar{S}_{ij}}, \qquad \bar{\Omega}^* = \frac{k}{\varepsilon}\sqrt{2\bar{\Omega}_{ij}\bar{\Omega}_{ij}} \tag{13}$$

The non-constant coefficients used here are the following [25][34]:

$$C_\mu = \frac{C_{a0}}{C_{a1} + C_{a2}\bar{S}^* + C_{a3}\bar{\Omega}^*} \tag{14}$$

$$C_1 = \frac{C_{NL1}}{(C_{NL6} + C_{NL7}\bar{S}^{*3})C_\mu} \tag{15}$$

$$C_2 = \frac{C_{NL2}}{(C_{NL6} + C_{NL7}\bar{S}^{*3})C_\mu} \tag{16}$$

$$C_3 = \frac{C_{NL3}}{(C_{NL6} + C_{NL7}\bar{S}^{*3})C_\mu} \tag{17}$$

$$C_4 = C_{NL4}C_\mu^2 \tag{18}$$

$$C_5 = C_{NL5}C_\mu^2 \tag{19}$$

The model constants used in the formulations above, and adapted from [25], are reported in Table I.

Table I. Cubic NLEVM constants

C_{a0}	C_{a1}	C_{a2}	C_{a3}	C_{NL1}	C_{NL2}	C_{NL3}	C_{NL4}	C_{NL5}	C_{NL6}	C_{NL7}
0.667	3.9	1.0	0.0	0.8	11.0	4.5	-5.0	-4.5	1000.0	1.0

2.3. WALE LES closure

The wall-adapting local eddy-viscosity (WALE) turbulence model is a subgrid scale (SGS) closure introduced by Nicoud and Ducros [35] with the goal of improving the wall behavior of classic LES closures. It does not require explicit filtering, and models the turbulent viscosity taking into account both the resolved strain and rotation rate, instead of the strain rate only. The residual stress tensor is modeled using the Boussinesq relation, where a variable eddy viscosity is used:

$$\nu_t = (C_w\Delta)^2 \frac{\left(\bar{S}_{ij}^d\bar{S}_{ij}^d\right)^{3/2}}{\left(\bar{S}_{ij}\bar{S}_{ij}\right)^{5/2} + \left(S_{ij}^d S_{ij}^d\right)^{5/4}} \tag{20}$$

A suitable value for C_w may range between 0.55 and 0.60 [35]; 0.544 was used in this work. The tensor $\bar{S}_{ij}^d$ is defined as:

$$\bar{S}_{ij}^d = \bar{S}_{ik}\bar{S}_{kj} + \bar{\Omega}_{ik}\bar{\Omega}_{kj} + \frac{2}{3}\delta_{ij}(\overline{II}) \tag{21}$$

Where $\overline{II}$ is the second principal invariant of the resolved velocity gradient tensor, defined as:

$$\overline{II} = -\frac{1}{2}\frac{\partial \bar{u}_i}{\partial x_j}\frac{\partial \bar{u}_j}{\partial x_i} = \frac{1}{2}(\bar{\Omega}_{mn}\bar{\Omega}_{mn} - \bar{S}_{mn}\bar{S}_{mn}) \tag{22}$$

2.4. STRUCT approach

The STRUCT model is a hybrid turbulence approach recently proposed by Lenci and Baglietto [24]. It aims at overcoming the weaknesses of URANS in the simulation of industrial unsteady flows, while maintaining robustness and feasible grid requirements for large-scale applications. It is recognized that URANS is not suitable for complex flows with strong resolved flow deformation. This is characterized for example by large values of $\bar{\Omega}^*$ or $\bar{S}^*$. In such cases, lack of scale separation exists between large-scale and residual velocity fluctuations. This violation of the URANS assumption introduces significant inaccuracy.

The STRUCT approach leverages the eddy-viscosity prediction of NLEVMs as described in Section 2.2, and identifies topological structures where local resolution of turbulence is desirable. Regions of high deformation are described using the second principal invariant of the resolved velocity gradient tensor, $\overline{II}$. This parameter takes into account both strain and rotation-dominated structures in the resolved flow, and shares some similarities with the concept of coherent structures in the instantaneous field.

In the current version of the STRUCT model, the residual stress anisotropy tensor is defined as in (9), using for the eddy viscosity the following step function:

$$\nu_t = \begin{cases} \nu_t & f_r < f_{r,0} \\ \phi\nu_t & f_r \geq f_{r,0} \end{cases} \tag{23}$$

Where f_r is a characteristic frequency of the resolved flow, defined as:

$$f_r = \sqrt{|\overline{II}|} \tag{24}$$

The definition in (23) is used to identify regions of poor scale separation. Those are described as the regions where the characteristic frequency of resolved flow described as in (24) is higher than a local value $f_{r,0}$, representative of the frequency of the modeled flow. The work in [24] presents the general concept of the STRUCT model, while the authors are currently developing a complete formulation aiming at providing closed flow-dependent functions for $f_{r,0}$ and ϕ. In the current formulation, which has been presented for the validation of the concept, those parameters are set as constant.

3. COMPUTATIONAL DETAILS

3.1. Flow case description

The triple-jet experiment performed by Tokuhiro and Kamide [13], shown in figure 1, utilized a large tank for the mixing of three jets of fluid at two different temperatures. Blocks were used to create rectangular inlet flows. The jets were bounded on two sides by separation plates extending far enough to isolate the flow in the mixing area of study. The experiment was conducted at a range of temperatures, delta temperatures, and velocities. In this study, we consider only the case where the temperature of the jets are 25 °C and 30 °C, and velocities of all jets are 0.5 m/s. The Reynolds number at the outlet of the center nozzle, calculated using the hydraulic diameter of the inlet jet, is $\mathrm{Re} = 1.8 \times 10^4$ [13]. Velocity profiles

were measured with an ultrasound Doppler velocimetry (UDV) system, while temperature profiles were measured using a traversing tree with 39 thermocouples.

Nishimura and Kimura [21] determined that the standard *k-ε* turbulence model is unable to capture the highly turbulent and unsteady nature of the flow. They introduced the LRSFM model, which showed higher, although limited, accuracy in flow description. Kimura, Nishimura, and Kamide [20] further studied these models and showed that quasi-direct numerical simulation (Q-DNS) can accurately describe the time-averaged temperature field, and is able to generally match the trend of the temperature fluctuation power spectrum density. Q-DNS refers to the solution of the momentum equation with no closure, hence zero residual stress terms. Due to the success of no closure methods in past work, in our flow description comparisons below we include results obtained with this approach. Jung and Yoo [23] and Cao, Lu, and Lv [22] demonstrated the success of LES methods for this geometry.

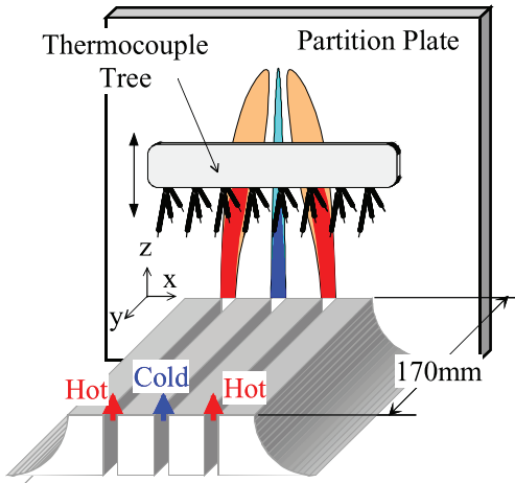

Figure 1. Schematic of the experimental setup. There are partition plates on each side of the inlet blocks. Figure from Kimura et al. [36]**.**

To this point, no URANS-based methods have shown general success and applicability to experimental thermal striping flows, which is necessary for full-scale reactor coolant simulations.

3.2. Numerical Methods

All analyses are performed using the commercially available finite-volume CFD code STAR-CCM+ version 9.04.011, while a development version is adopted for implementation of the STRUCT model. A segregated flow solver based on the SIMPLE algorithm applied on co-located variables with Rhie-Chow interpolation is leveraged. The segregated fluid energy formulation is used, which solves an additional transport equation as part of the SIMPLE iterations, according to which temperature is determined [37]. The Boussinesq approximation is adopted to account for the effects of buoyancy, following the approach of Durve et. al [38], and owing to the small density variation for water between 25 °C and 30 °C (< 0.1%). All convective terms are approximated with an upwind-based non-oscillatory 2nd order scheme, using the Venkatakrishnan reconstruction gradient limiting. For LES simulations, a locally-bounded central-differencing scheme is adopted for the convective terms. The Hybrid Gauss LSQ gradient reconstruction method with 2nd order time integration is used. The time step for each case is determined by the requirement of Courant number lower than 1.

3.3. Computational Grid

The computational domain is simplified to include only the regions of interest in the experimental setup and is shown in figure 2. The size of the simulated region is 300(x) x 60(y) x 600(z) mm plus three identically sized inlet channels measuring 20(x) x 60(y) x 600(z) mm. The inlet channels are extruded to 600 mm to create fully developed profiles in the simulation. A fine 1 mm computational grid was created as optimal mesh for LES simulations, while a coarse 4 mm grid was created on which to compare all the turbulence models. Tests on even coarser grids, not shown here, confirmed that sufficient grid convergence is achieved for the URANS and STRUCT models in the 4 mm grid. The wall function utilized requires a non-dimensional y^+ value over 30. This requirement is satisfied with a 4 mm cell at the wall.

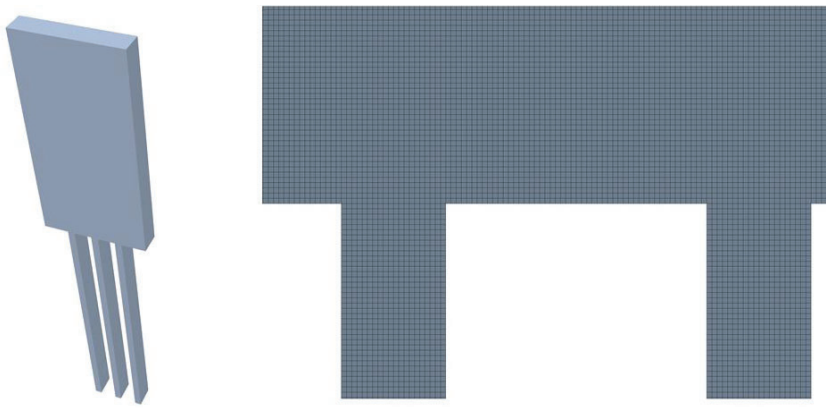

Figure 2. Computational domain, and detail of the 1 mm isotropic hexahedral trimmed mesh

3.4. Boundary conditions

A flat velocity profile of 0.5 m/s is used at the inlet of the extruded channels as boundary condition. The inlet temperature is specified as 25 °C in the central channel and 30 °C at the two sides. The walls in the experiment are set as no-slip boundary conditions, while the two lateral and ceiling boundaries are set as specified pressure boundaries. The entire region is initialized to the mean mass flow mixing temperature of 28.33 °C, and the same temperature is used for reverse flow at the pressure outlets. Other parameters used for such reverse flow are a turbulence intensity of 0.25 and a turbulent viscosity ratio of 90, as determined during separate test simulations.

A sensitivity study performed on this case reached the conclusion that for the lateral sides of the domain a boundary condition with specified pressure, is the most appropriate. The boundary condition specifies the pressure on the boundary, and reconstructs the velocities. This avoids asymmetric solutions found using other boundary conditions that compromise the results far from the wall. Additionally, the inlet boundaries were extruded to create fully developed flow conditions.

4. RESULTS AND DISCUSSION

The turbulence closure approaches illustrated in Section 2 plus an unclosed Q-DNS formulation, as discussed in Section 3.1, are tested on the coarse mesh, while LES is also tested on the fine mesh. Parameters used for the STRUCT approach are $\phi = 1 \times 10^{-5}$ and $f_{r,0}$ = 1.4 Hz. The latter parameter has been chosen as a representative value of the ε/k modeled frequency scale resulting from URANS.

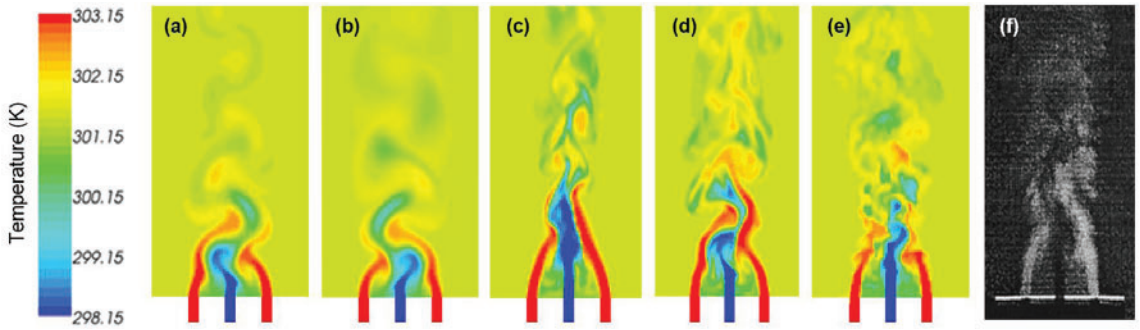

Figure 3. Instantaneous temperature distribution: (a) Realizable k-ε, (b) cubic k-ε (c) no-closure (d) STRUCT (e) LES (f) Experiment figure (f) taken from [13]

Results obtained using the STRUCT approach show higher accuracy over all forms of URANS tested, and improvement over LES. Results are presented on the same figures to appreciate trends more clearly, in comparison to experimental data. All simulation results reported are taken at the mid-plane location, between the two isolation plates. Figure 3 depicts the instantaneous temperature profiles along with an image of the flow extracted from the experiment.

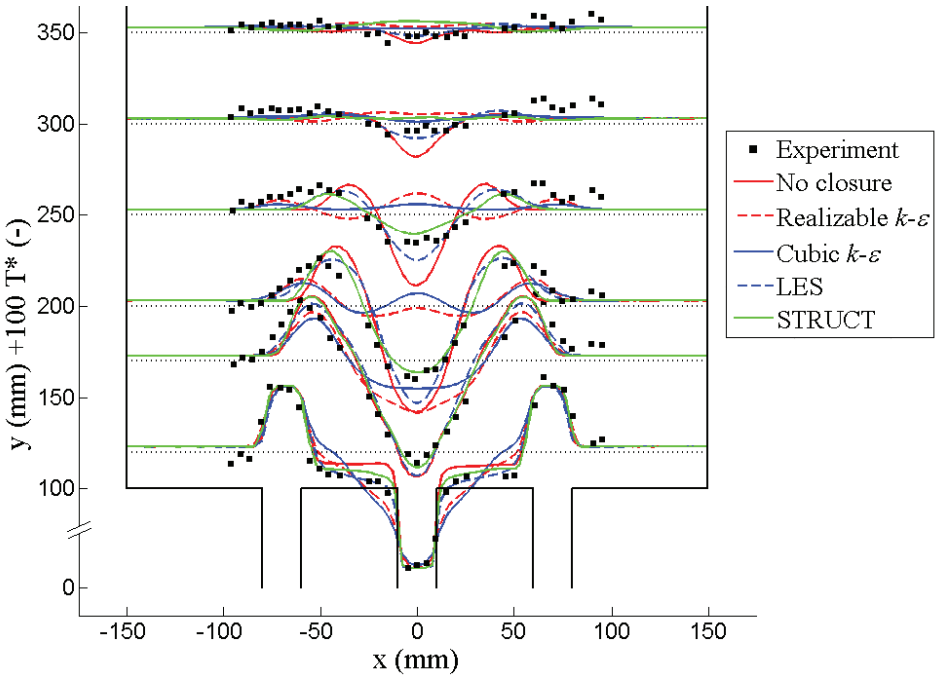

Figure 4. Time averaged temperature profiles for the 4 mm mesh.

Figure 4 shows the time-averaged temperature profiles for the different models tested. It is interesting to note that LES provides an accurate description of temperature, velocity and temperature fluctuation profiles not only on the fine 1 mm mesh (not shown in the figure), but also in the coarse 4 mm mesh, which is in agreement with previous tests [39]. However, as it will be shown later in Figure 7, only the fine-mesh LES predicts the temperature fluctuation frequency. This parameter is very important in thermal striping analysis, and indicates that the apparently accurate profile prediction from the coarse-mesh LES could be an artifact of the averaging process, rather than a reliable LES result.

In figures 4, 5, and 6 we only plot the 4 mm results for the LES simulations, since we observed that for those parameters, results are very close to those of the 1 mm case. The LES and the STRUCT methods match the experimental data much closer than other approaches, which introduce a significant error either in the lower (URANS) or middle (no closure/Q-DNS) part.

Time-averaged velocity profiles have been plotted in Figure 5. All models are able to successfully predict the velocity profiles at all data levels except for the 2nd and 3rd level, which correspond to the heights at which most mixing is experimentally observed. At these heights, a behavior of both URANS models, i.e. the realizable *k-ε* and the cubic *k-ε*, to over predict mixing is observed, showing a flattening of the velocity profile much earlier than what is measured. The LES, STRUCT, and no-closure methods can successfully capture the behavior on the 2nd data level, while over predicting the velocity gradients on the third level. At this height, only the STRUCT method captures the velocity above the center jet, while slightly over predicting the one above the outer jets.

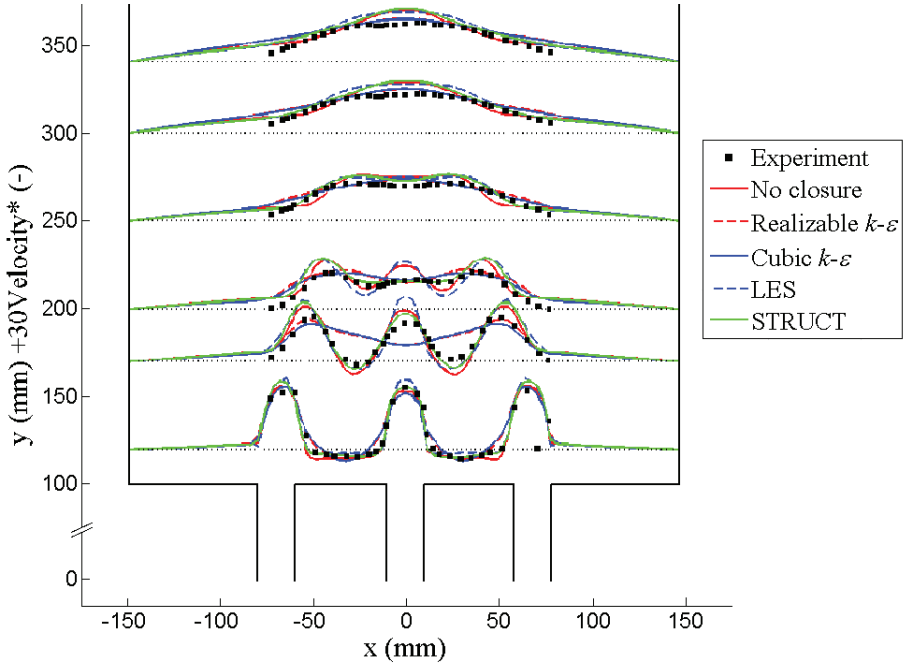

Figure 5. Time averaged velocity profiles for the 4 mm mesh.

The normalized temperature fluctuation intensity is of significant importance to thermal striping analysis because it is the mechanism by which temperatures are absorbed by the surrounding materials. Profiles are plotted in Figure 6. The dimensionless temperature used is defined in (25), where T_h, T_c and T_{avg} are respectively the temperature of the hot inlets, the cold inlet, and the mass flow rate weighted average.

$$T^* = \frac{T - T_{avg}}{T_h - T_c} \tag{25}$$

The realizable and cubic *k-ε* models strongly over predict the temperature fluctuations at the lowest levels. The LES, STRUCT, and no-closure methods all capture the experimental fluctuations at the lower levels, while slightly over predicting fluctuations at the higher ones. An over prediction of fluctuations at the center

is shown in the result with no closure at the upper level. During grid convergence tests performed on very coarse meshes we observed that LES and URANS models struggle to accurately predict time-averaged flow profile quantities. In those cases, the STRUCT model has shown to provide results less accurate than for the fine case, but still consistently closer to the experiments than the ones obtained with URANS, demonstrating robustness. For the very coarse 7 mm mesh tested, STRUCT results seem very close to URANS ones, and future work is needed to demonstrate its behavior in the coarse mesh limit.

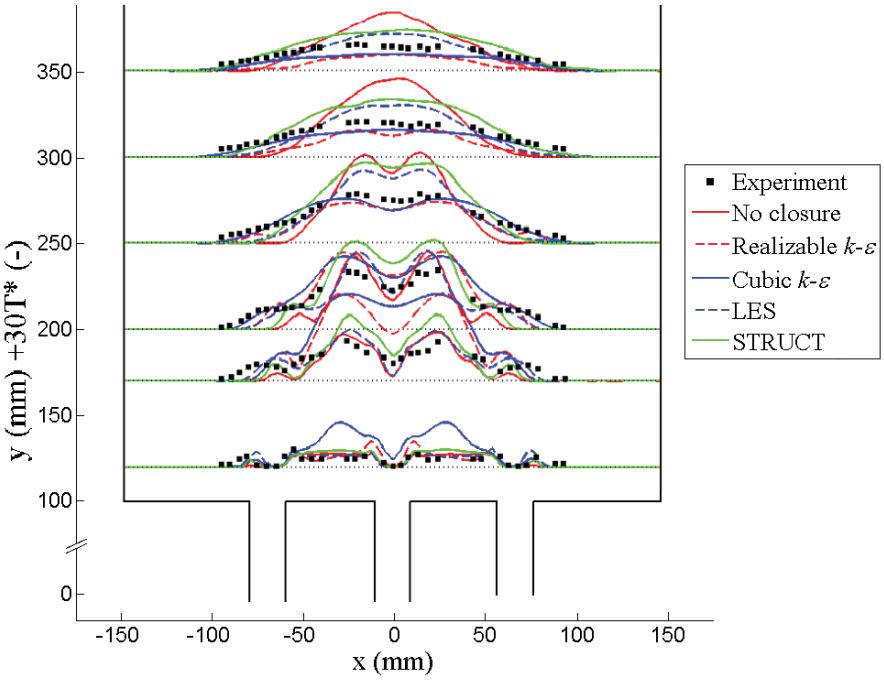

Figure 6. Time averaged normalized temperature fluctuation intensity on the 4 mm mesh.

Finally, the dominant frequencies of temperature fluctuation are of critical importance for determining the attenuation of temperature variation in materials. To clarify, these frequencies are not related to the characteristic frequency introduced in the STRUCT model. The normalized power spectral densities of the different models at the experimental measuring point, x = -15 mm, y = 0 (centerline), z = 100 mm, are shown in figure 7. The experiment yields a dominant frequency of approximately 2.3 Hz. This value is best predicted by the cubic *k-ε* (~2.28 Hz) and the STRUCT approach (~2.38 Hz). The realizable *k-ε* and the no-closure method both provide a significantly inaccurate dominant frequency. The fine-mesh LES predicts the fluctuation frequency within 5% to about 2.45 Hz. However, lack of accuracy of the coarse mesh LES is evidenced by many dominant frequencies, all of which poorly match the observed frequency. As already mentioned, this result is particularly interesting, because although LES on coarse grids can predict the time-averaged flow profiles, it fails to capture the frequencies of fluctuation, which are of paramount importance to material degradation due to thermal striping. The reason for this failure is thought to be the application of a too coarse LES filter width.

We conclude that on the 4 mm mesh, results obtained with the STRUCT approach are the ones that most closely match the experimental description of thermal striping. No increase in accuracy is expected or sought after with respect to LES on suitable grids. Additional work should aim at achieving and testing the optimal performance and robustness of the STRUCT model in the fine and coarse-mesh limits.

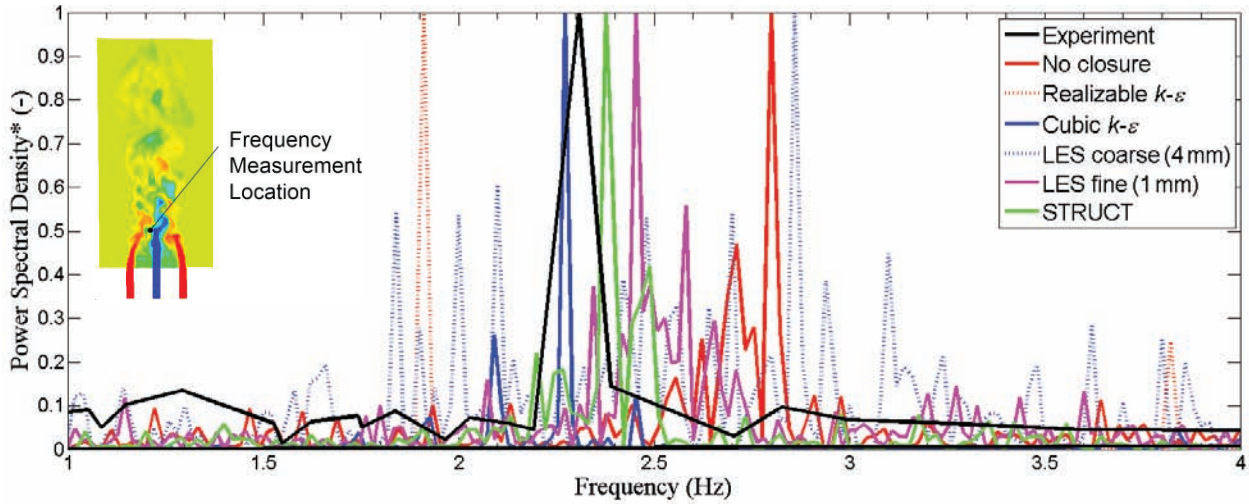

Figure 7. Normalized power spectral densities of temperature fluctuation. All models are applied to the coarse (4 mm) mesh, except for LES, which is applied to both meshes, as defined in the legend.

5. CONCLUSIONS

Several turbulence models have been tested against experimental data from the well-established Tokuhiro and Kimura triple-jet test case, in order to assess their applicability to predicting thermal striping in sodium fast reactors. The two URANS models tested, a linear realizable k-ε and a cubic k-ε, confirmed what was observed by other authors, i.e. limited accuracy in the prediction of temperature, velocity, and temperature fluctuation profiles in the regions of significant mixing. The STRUCT hybrid approach has shown to systematically produce results significantly closer to the experimental data. The time-averaged flow prediction capabilities of the LES and the STRUCT model are considerably more accurate than the URANS predictions. The LES model delivers accurate results on relatively coarse computational grids in terms of flow profile prediction but fails to predict the frequencies of fluctuation. The STRUCT approach is the only model among the ones tested on the 4 mm coarse grid that was capable of predicting the experimental profiles of the time-averaged temperature and velocity, the temperature fluctuation and the frequency of temperature fluctuations.

The STRUCT approach shows considerable promise in modelling the behavior of thermal striping. It is able to combine the accuracy of flow profile prediction on coarse grids, with the accurate prediction of frequencies involved in temperature fluctuations. Additionally, on the very coarse meshes tested for grid convergence analysis, STRUCT has shown to consistently provide more accurate results than URANS, ensuring robustness equivalent to URANS methods. Computational tests have shown that the STRUCT method on the URANS grids represents a speedup of over 70 times over the fine-grid LES, while requiring an increase in computational cost of only 10-20% over URANS models. Future work will focus on the completion of the model and will extend the validation of the STRUCT approach with the aim of identifying practical guidelines for robust industrial application of full-scale SFR simulations.

NOMENCLATURE

The nomenclature used in this paper is shown in Table II. Vectors are marked with one subscript index, second-order tensors with two subscript indices, and scalars with none. Einstein's notational convention for summation is adopted for the sake of brevity.

Table II. Nomenclature

Notation	Unit (SI)	Definition	Notation	Unit (SI)	Definition
A	–	Coefficient	$\bar{S}_{ij}$	s^{-1}	Mean rate of strain tensor
a_{ij}	J kg^{-1}	Residual stress anisotropy tensor	$\bar{S}^*$	–	Dimensionless mean rate of strain tensor
C	–	Coefficient	σ	–	Effective turbulent Prandtl number
Δ	m	Grid size	$\bar{S}_{ij}^d$	s^{-2}	Tensor used in the WALE model
δ_{ij}	–	Kronecker delta	T	K, °C	Temperature
ε	W kg^{-1}	Turbulence dissipation rate	T^*	–	Dimensionless temperature
f_r	s^{-1}	Characteristic frequency of the resolved flow	τ_{ij}	J kg^{-1}	Residual stress tensor
$\overline{II}$	s^{-2}	Second invariant of the mean velocity gradient tensor	U^*	s^{-1}	Parameter in the WALE model
k	J kg^{-1}	Turbulence kinetic energy	u_i	m s^{-1}	Velocity
ν	m^2s^{-1}	Kinematic molecular viscosity	y^+	–	Dimensionless distance from the wall
ν_t	m^2s^{-1}	Kinematic turbulence eddy viscosity	ϕ	–	Damping coefficient
P_k	W kg^{-1}	Production of turbulence kinetic energy	x_i	m	Position
p	Pa	Static pressure	$\bar{\Omega}_{ij}$	s^{-1}	Mean rate of rotation tensor
ρ	kg m^{-3}	Density	$\bar{\Omega}^*$	–	Dimensionless mean rate of rotation tensor

ACKNOWLEDGMENT

The authors would like to acknowledge TerraPower for providing financial support for this project.

REFERENCES

[1] O. Gelineau and M. Sperandio, "Thermal fluctuation problems encountered in LMFBRs," in *Specialistic Meeting "Correlation Between Material Properties and Thermohydraulics Conditions in LMFBRs"1994.*
[2] J. Brunings, "LMFBR Thermal-Striping Evaluation," Canoga Park, California, 1982.
[3] Tenchine and Nam, "The Thermal Hydraulics of Coaxial Sodium Jets," *AiChE Symp. Ser.*, vol. 83, no. 257, pp. 151–156, 1987.
[4] S. Moriya and I. Ohshima, "Hydraulic similarity in the temperature fluctuation phenomena of non-isothermal coaxial jets," *Nucl. Eng. Des.*, vol. 120, pp. 385–393, 1990.
[5] N. Hattori, Y. Arai, A. Sugiyama, K. Koyabu, and M. Hirakawa, "Experimental Study of Coaxial Double Pipe Air Jets at Different Temperatures," *Heat Transf. - Japanese Res.*, vol. 27, no. 6, pp. 431–446, 1998.
[6] M. Wakamatsu, H. Nei, and K. Hashiguchi, "Attenuation of Temperature Fluctuations in Thermal Striping," *J. Nucl. Sci. Technol.*, vol. 32, no. November 2013, pp. 752–762, 1995.
[7] T. Kawamura, K. Shiina, M. Ohtsuka, and I. Tanaka, "Experimental Study on Thermal Striping in Mixing Tees with Hot and Cold Water," in *ICONE10*, 2002.
[8] K. Yuki, H. Hashizume, M. Tanaka, and T. Muramatsu, "Investigation of Thermal Hydraulic Mixing Mechanism in T-junction Pipe with a 90-degree Bend in Upstream Side for Mitigation and Controlling of Thermal-striping Phenomena," 2006.
[9] L. W. Hu and M. S. Kazimi, "LES benchmark study of high cycle temperature fluctuations caused by thermal striping in a mixing tee," *Int. J. Heat Fluid Flow*, vol. 27, pp. 54–64, 2006.
[10] H. Kamide, M. Igarashi, S. Kawashima, N. Kimura, and K. Hayashi, "Study on mixing behavior in a tee piping and numerical analyses for evaluation of thermal striping," *Nucl. Eng. Des.*, vol. 239, pp. 58–67, 2009.
[11] J. I. Lee, L. W. Hu, P. Saha, and M. S. Kazimi, "Numerical analysis of thermal striping induced high cycle thermal fatigue in a mixing tee," *Nucl. Eng. Des.*, vol. 239, pp. 833–839, 2009.
[12] P. Chellapandi, S. C. Chetal, and B. Raj, "Thermal striping limits for components of sodium cooled fast spectrum reactors," *Nucl. Eng. Des.*, vol. 239, pp. 2754–2765, 2009.

[13] A. Tokuhiro and N. Kimura, "Experimental investigation on thermal striping. Mixing phenomena of a vertical non-buoyant jet with two adjacent buoyant jets as measured by ultrasound Doppler velocimetry," *Nucl. Eng. Des.*, vol. 188, pp. 49–73, 1999.
[14] S.-K. Choi and S.-O. Kim, "Evaluation of Turbulence Models for Thermal Striping in a Triple Jet," *J. Press. Vessel Technol.*, vol. 129, p. 583, 2007.
[15] M. Crosskey and A. Ruggles, "UTK Twin Jet Water Facility Computational Fluid Dynamics Validation Data Set," in *Proceedings of ICAPP 2014*, 2014, pp. 1940–1945.
[16] O. Omotowa, R. Skifton, and A. Tokuhiro, "Benchmark Studies of Thermal Jet Mixing in SFRs Using a Two- Jet Model," in *Proceedings of ICAPP 2012*, 2012, pp. 2296–2301.
[17] D. Lu, Q. Cao, J. Lv, and Y. Xiao, "Experimental study on three-dimensional temperature fluctuation caused by coaxial-jet flows," *Nucl. Eng. Des.*, vol. 243, pp. 234–242, 2012.
[18] S. Lomperski, E. Merzari, A. Obabko, W. D. Pointer, and P. Fischer, "The MAX Facility for CFD Code Validation," in *Proceedings of ICAPP 2012*, 2012, pp. 1873–1879.
[19] M. Nishimura, A. Tokuhiro, N. Kimura, and H. Kamide, "Numerical study on mixing of oscillating quasi-planar jets with low Reynolds number turbulent stress and heat flux equation models," *Nucl. Eng. Des.*, vol. 202, pp. 77–95, 2000.
[20] N. Kimura, M. Nishimura, and H. Kamide, "Study on Convective Mixing for Thermal Striping Phenomena. Experimental Analyses on Mixing Process in Parallel Triple-Jet and Comparisons between Numerical Methods.," *JSME International Journal Series B*, vol. 45. pp. 592–599, 2002.
[21] M. Nishimura and N. Kimura, "URANS computations for an oscillatory non-isothermal triple-jet using the k-ε and second moment closure turbulence models," *Int. J. Numer. Methods Fluids*, vol. 43, no. March 2002, pp. 1019–1044, 2003.
[22] Q. Cao, D. Lu, and J. Lv, "Numerical investigation on temperature fluctuation of the parallel triple-jet," *Nucl. Eng. Des.*, vol. 249, pp. 82–89, 2012.
[23] J. H. Jung and G. J. Yoo, "Analysis of Unsteady Turbulent Triple Jet Flow with Temperature Difference," *J. Nucl. Sci. Technol.*, vol. 41, no. November 2014, pp. 931–942, 2004.
[24] G. Lenci and E. Baglietto, "A structure-based approach for topological resolution of coherent turbulence: concept overview," in *16th International Topical Meeting on Nuclear Reactor Thermal Hydraulics (NURETH-16)*, 2015.
[25] E. Baglietto and H. Ninokata, "Anisotropic Eddy Viscosity Modeling for Application to Industrial Engineering Internal Flows," *Int. J. Transp. Phenom.*, vol. 8, no. 2, pp. 85–101, 2006.
[26] M. Germano, "Turbulence: the filtering approach.," *J. Fluid Mech.*, vol. 238, pp. 325–336, 1992.
[27] B. J. Perot and J. Gadebusch, "A self-adapting turublence model for flow simulation at any mesh resolution.," *Phys. Fluids*, vol. 19, pp. 1–11, 2007.
[28] W. Jones and B. Launder, "The prediction of laminarization with a two-equation model of turbulence," *Int. J. Heat Mass Transf.*, vol. 15, no. 2, pp. 301–314, 1972.
[29] B. Launder and D. Spalding, "The numerical computation of turbulent flows," *Comput. Methods Appl. Mech. Eng.*, vol. 3, no. 2, pp. 269–289, 1974.
[30] T. H. Shih, W. W. Liou, A. Shabbir, Z. Yang, and J. Zhu, "A new k-ϵ eddy viscosity model for high reynolds number turbulent flows," *Comput. Fluids*, vol. 24, no. 3, pp. 227–238, 1995.
[31] S. B. Pope, "A more general effective-viscosity hypothesis," *J. Fluid Mech.*, vol. 72, no. 2, p. 331, 1975.
[32] E. Baglietto and H. Ninokata, "Improved turbulence modeling for performance evaluation of novel fuel designs," *Nucl. Technol.*, vol. 158, no. 2, pp. 237–248, 2007.
[33] T. Shih, J. Zhu, and J. Lumley, "A new Reynolds stress algebraic equation model," *Comput. Methods Appl. Mech. Eng.*, 1995.
[34] F. Lien, W. Chen, and M. Leschziner, "Low-Reynolds-number eddy-viscosity modelling based on non-linear stress-strain/vorticity relations," in *Proceedings of the 3rd symposium on Engineering turbulence modelling and Experiments*, 1996, pp. 91–100.
[35] F. Nicoud and F. Ducros, "Subgrid-Scale Stress Modelling Based on the Square of the Velocity Gradient Tensor," pp. 183–200, 1999.
[36] N. Kimura, H. Kamide, P. Emonot, and K. Nagasawa, "Study on Thermal Striping Phenomena in Triple-Parallel Jet - Investigation on Non-Stationary Heat Transfer Characteristics Based on Numerical Simulation -," 2007.
[37] CD-adapco, "User Guide, STAR-CCM+ Version 9.04," 2014.
[38] A. Durve, A. W. Patwardhan, I. Banarjee, G. Padmakumar, and G. Vaidyanathan, "Thermal striping in triple jet flow," *Nucl. Eng. Des.*, vol. 240, no. 10, pp. 3421–3434, 2010.
[39] S. Chacko, Y. M. Chung, S. K. Choi, H. Y. Nam, and H. Y. Jeong, "Large-eddy simulation of thermal striping in unsteady non-isothermal triple jet," *Int. J. Heat Mass Transf.*, vol. 54, pp. 4400–4409, 2011.